Topographic Normalization of Landsat Thematic Mapper Digital Imagery

Daniel L. Civco
Laboratory for Remote Sensing, Department of Natural Resources Management and Engineering, The University of Connecticut, U-87, Room 308, 1376 Storrs Road, Storrs, CT 06269-4087

ABSTRACT: A two-stage technique is described for the removal of the topographic effect from Landsat Thematic Mapper digital image data. The topographic effect is caused by differential solar illumination of the Earth's surface in undulating terrain. This effect often results in widely varying spectral responses from what are perceived as uniform cover types, which can confound image processing operations such as supervised classification, cluster analysis, and scene segmentation. The process described in this paper, which requires the use of a digital elevation model registered to Landsat TM image data, reduces most of this topographic effect and enables the generation of images with more uniform multispectral response properties. Normalization of Landsat TM radiance data reduced variance, introduced by the topographic effect, by as much as 69 percent. Reduction of the topographic effect in satellite digital multispectral data will improve the overall computer-assisted mapping process.

INTRODUCTION

WHILE THERE IS AN EXPECTED DEGREE of natural spectral variability within any particular cover class, that introduced by topographic slope and aspect is artificial in the sense that illumination of and radiance from features on a plane not normal to the source of irradiance do not accurately represent the true spectral response properties of those features. For example, for Landsat data this generally results in darker slopes facing away from the sun and brighter sun-facing slopes. This effect is amplified under low sun angle conditions in areas of substantial topographic relief, and for a Lambertian assumption, can be modeled after the cosine law of spherical geometry (*cf.* Sellers, 1972):

$$\gamma = \cos\theta_0 \cos\theta_n + \sin\theta_0 \sin\theta_n \cos(\phi_n - \phi_0) \qquad [1]$$

where

γ = cosine angle between solar incident angle and the local surface normal,
θ_0 = solar zenith angle,
θ_n = zenith angle of the normal to the surface,
ϕ_0 = solar azimuth angle, and
ϕ_n = topographic aspect angle.

The so-called topographic effect poses several problems in computer-assisted analysis of digital remote sensing data, especially for automated land-cover classification (Cicone *et al.*, 1977; Woodcock *et al.*, 1980) and image segmentation (i.e., the partitioning of a scene into regions of spectrally homogeneity).

One of the earliest attempts to simulate and quantify this topographic effect involved the measurement of differential spectral radiance from a uniform sand surface under various slope and angle combinations (Holben and Justice, 1980). It was found that the magnitude of the topographic effect varied as a function of the solar inclination and azimuth and the terrain's degree of slope and orientation, and that this effect can produce wide variations in the radiance associated with a perceived uniform (*i.e.*, homogeneous) cover type. Based in this simulation study, it was suggested that a model should be developed that would incorporate solar and terrain geometries to reduce the topographic effect, which, in theory, would improve automated multispectral classification.

A number of investigations which attempt to explain the topographic effect, especially for Landsat and SPOT digital multispectral data, have recently been conducted (Hall-Konyves, 1987; Jones *et al.*, 1988; Kawata *et al.*, 1988; Leprieur *et al.*, 1988; Shasby and Carneggie, 1986; Teillet *et al.*, 1982). Most of these studies attempted to account for and correct the negative aspects associated with the topographic effect by modifying the surface radiance values recorded by the satellite sensors using the cosine of the angle of incidence of the solar beam with a pixel's topographic degree of slope and inclination, as calculated from a registered digital elevation data set. Some of the more significant observations and findings stemming from these research projects are

- digital elevation data of a resolution comparable to the multispectral data being corrected should be used in the modeling process (Kawata *et al.*, 1988);
- in correcting for the topographic effect under a Lambertian surface assumption, images tended to be over-corrected, with slopes facing away from the sun (i.e., northerly-facing slopes in the northern hemisphere) appearing brighter than sun-facing slopes (i.e., southerly-facing slopes) of similar cover composition, indicating that the correction is less than γ - the cosine of the incidence angle (Jones *et al.*, 1988)-especially under conditions of low γ (Kawata *et al.*, 1988);
- the technique of dividing radiance values by the cosine of the solar incidence angle increased the variance associated with individual, *perceived uniform* cover types (Holben and Justice, 1980);
- most techniques consider only the direct solar beam contribution to irradiance, and hence radiance, but that the diffuse component is also affected by local topography (Hall-Konyves, 1987);
- there is often strong anisotropy of apparent reflectance, which is wavelength dependent, and that solar, surface, and sensor geometry should be considered in the modeling process (Leprieur *et al.* 1988);
- the amount of correction required is a function of wavelength (Holben and Justice, 1980) and that particular attention should be given to the middle infrared wavelengths (Leprieur *et al.*, 1988; Kawata *et al.*, 1988); and
- the topographic effect could not be removed completely from severely shadowed areas such as deep valleys (Kawata *et al.*, 1988).

The relative over- and under-illumination associated with the topographic effect has been observed to be particularly pronounced in Landsat Thematic Mapper imagery acquired in late fall, winter, and spring seasons of the glaciated northeastern United States — periods when, at this mid-latitude, deciduous trees are leafless and radiance data are a combination of forest canopy and sub-canopy (*i.e.*, surface) reflectance properties. For example, in terms of supervised classification problems, pixels from northerly-facing deciduous forested slopes exhibit reflec-

PHOTOGRAMMETRIC ENGINEERING AND REMOTE SENSING,
Vol. 55, No. 9, September 1989, pp. 1303–1309

0099-1112/89/5509–1303$02.25/0

tances lower than the overall true reflectance for this cover type and are often misclassified as a wetland category. Also, pixels from southerly-facing deciduous forested slopes exhibit reflectances higher than the mean reflectance for the class and are often falsely allocated to a non-forest category, such as fallow pastures or barren land. Further, because of the exaggerated variance introduced by the topographic effect, unsupervised classification tends to produce a number of spectral clusters far in excess of the true number of informational classes. Similarly, image segmentation of scenes with a substantial topographic effect tends to produce overly partitioned images.

Objective

The objective of this study was to develop a technique that would remove much of the topographic effect present in Landsat Thematic Mapper digital image data, while at the same time preserving the overall spectral characteristics of the scene being corrected. Emphasis was placed on removing this effect in images with low sun angle conditions and in areas of substantial topographic relief covered principally by leafless deciduous forest where the topographic effect is particularly pronounced. This technique was developed as part of a larger research effort addressing the improvement of accuracy of the information derived from Landsat Thematic Mapper data (Civco and Kennard, 1988). This project deals with advanced methods for computer-assisted extraction of land use and land cover from such digital imagery and incorporates both spectral and spatial attributes as well as artificial intelligence techniques in scene segmentation and classification (*cf.*, Civco, 1987; Civco 1989). Toward this end, a topographic normalization technique was designed and applied to two dates of Landsat TM imagery.

Study Area

The study area for this research was the town of North Stonington, Connecticut, located in the state's Eastern Highlands. North Stonington is an inland rural community of approximately 138.8 km^2(53.6 mi^2) with a population of nearly 4,300. Its landscape is dominated by forest, agricultural, and inland wetland cover types. Although largely forested, there are substantial agricultural lands in the town, consisting principally of corn, pasture and hay, and vineyards. Also, there has been recent significant residential growth because the town serves as a *bedroom community* for the greater Norwich-New London metropolitan area.

The geology of this area of southern New England is the product of glaciation and its landscape is characterized by peneplains, or sloping planes of hilltops. Post-glacial erosion has further modified this peneplain and has accentuated the differences between hilltops and valley bottoms. The topography is very undulating with slopes ranging from zero to more than 45 percent over an elevational range of approximately 8 metres above mean sea level to nearly 170 metres.

Data Types

The data used in this study consisted of two dates of Landsat Thematic Mapper digital imagery:

- 24 March 1987; Path 12, Row 31; Scene ID 85111814491X0 and
- 11 May 1987; Path 12, Row 31; Scene ID 85116614504X0;

30-metre resolution digital elevation model (DEM) data, acquired from the United States Geological Survey (USGS) for four 7½-minute quadrangles:

- Ashaway,
- Jewett City,
- Old Mystic, and
- Voluntown;

and collateral information consisting of color infrared and black-and-white aerial photographs, black-and-white orthophotoquads, and topographic maps. These collateral data were used to identify the location and magnitude of the topographic effect and to assist in assessing the performance of the normalization process.

PROCEDURES

The PC ERDAS[1] remote sensing image processing system was used to perform all satellite and digital elevation data analyses. First, the Landsat TM data for both dates were extracted from computer compatible tapes (CCTs) for a window subsuming the town of North Stonington. Next, the two images were registered to one another with a subpixel precision (RMS = 0.50 pixel). Then, this composite, multidate image was geometrically corrected and projected into Universal Transverse Mercator (UTM) coordinates using a bilinear interpolation algorithm. Pixels were resampled to 30 metres to match the spatial characteristics of the digital elevation model (DEM) data.

The DEM data for the four topographic quadrangles bounding the study area were extracted individually from CCTs and spliced to form a single digital elevation composite. These 30-metre data were in the same geographic projection as the corrected TM data, and superimposition of the image and DEM data revealed registration between the two different data sets to be within one pixel. Because of both the banding and spurious data points introduced in the production of these DEMs, it was necessary to smooth the data with a low-pass filter. Two iterations of a 3 by 3 smoothing convolution were applied to the DEM data. This operation maintained the overall topographic structure of the data while at the same time removed much of the noise.

Shaded relief models, corresponding to the solar illumination conditions at the time of the Landsat overpass, were computed from the DEM data for each of the two dates of TM imagery used. The ephemeris information supplied with the Landsat TM CCTs provided the solar azimuth and altitude angles necessary to calculate this illumination model. This model is a special case of the application of the cosine law in which the resulting data, which in theory could range from -1.0 to +1.0, have been scaled over the 8-bit brightness range of the display device (0, 255 or 256 grey levels).[2] These shaded relief models were then extracted from the composite four-quadrangle data set for just the town by using a digitized polygon template of the study area.

A linear transformation of each of the original TM bands was then performed to derive *topographically normalized* images: i.e.,

$$\delta DN_{\lambda ij} = DN_{\lambda ij} + \left(DN_{\lambda ij} \times \frac{(\mu_k - X_{ij})}{\mu_k}\right) \quad [2]$$

where

$\delta DN\lambda_{ij}$ = the normalized radiance data for $pixel_{ij}$ in band λ,
$DN_{\lambda ij}$ = the *raw* radiance data for $pixel_{ij}$ in band λ,
μ_k = the mean value for the entire scaled (0, 255) illumination model, and
X_{ij} = the scaled (0, 255) illumination value for $pixel_{ij}$.

Applications of this *first stage normalization* algorithm to the TM data showed that variance was reduced while mean spectral responses were preserved. However, it was observed that the normalization was only partially successful in reducing the topographic effect – illumination and shadowing artifacts were not removed completely. Examination of the spectral signatures for several uniform categories for various slope-aspect conditions indicated that the first stage transformation proved to be inadequate – generally northerly slopes were still relatively darker

[1] Earth Resources Data Analysis System

[2] This is the default algorithm in ERDAS for the generation of shaded relief models.

and southern slopes brighter. This was confirmed by visual displays of various band combinations in which the topographic effect was still pronounced, particularly in the infrared bands.

In an effort to reduce the topographic effect further, an empirically-derived calibration coefficient was determined by comparing the spectral responses from large samples of an equal number of pixels (n = 1390) falling on northern and southern slopes with the overall mean spectral response for the category deciduous forest (n = 94,171). The differences in spectral response from a uniform mixed deciduous forest cover were determined by calculating the means and variances of pixels falling on both northerly- and southerly-facing slopes. The correction coefficient, C_λ, differed for each band and is based on the magnitude of adjustment (either upward or downward) to equalibrate the mean spectral response of the deciduous forest category: i.e.,

$$C_\lambda = \frac{[(\mu_\lambda - N_\lambda)/((\mu_\lambda - N_\lambda) - (\mu_\lambda - N'_\lambda)) + (\mu_\lambda - S_\lambda)/((\mu_\lambda - S_\lambda) - (\mu_\lambda - S'_\lambda))]}{2} \quad [3]$$

where

C_λ = the correction coefficient for band λ,
μ_λ = the overall mean for the deciduous forest category,
N_λ = the mean on northern slopes in the uncalibrated data,
N'_λ = the mean on northern slopes after the *first stage normalization*,
S_λ = the mean on southern slopes in the uncalibrated data, and
S'_λ = the mean on southern slopes after the *first stage normalization*.

In a linear transformation, similar to the first (Equation 2), these coefficients were used to correct further for the topographic effect present in the original (*i.e.*, raw) Landsat TM data: i.e.,

$$\delta DN_{\lambda ij} = DN_{\lambda ij} + ((DN_{\lambda ij} \times (\frac{(\mu_k - X_{ij})}{\mu_k})) \times C_\lambda) \quad [4]$$

where

$\delta DN\lambda_{ij}$ = the normalized radiance data for $pixel_{ij}$ in λ,
$DN_{\lambda ij}$ = the *raw* radiance data for $pixel_{ij}$ in band λ,
μ_k = the mean value for the entire scaled (0, 255) illumination model,
X_{ij} = the scaled (0, 255) illumination value for $pixel_{ij}$,
C_λ = an *empirically-derived* calibration coefficient for band λ.

In order to assess the validity of this modified version of the topographic effect correction algorithm, several measures were used:

- visual inspection of the original, *first stage* normalized, and *second stage* normalized TM images;
- a test of homogeneity by inspecting the means and standard deviations of the original, *first stage* normalized, and *second stage* normalized TM images; and
- a test of homogeneity by performing an unsupervised classification of the original, *first stage* normalized, and *second stage* normalized TM images.

RESULTS AND DISCUSSION

Plates 1 and 2 are color renditions of TM Bands 2, 3, and 4 of the March and May TM scenes, respectively, for the original and the first and second stage normalized images. Plates 1(a) and 2(a) of the original TM images graphically depict the topographic effect, especially in the northern (i.e., upper) portions of the images. The magnitude of the topographic effect is apparent in the original data, especially for steeply sloping deciduous forests located throughout the images, and particularly visible in the northwestern portions of the scenes. With the first stage normalization (Plates 1(b) and 2(b)) this effect is reduced while preserving the overall spectral characteristics of the image, but the tendency was toward under-correction. Table 1, which illustrates the calculation of the correction coefficient (C_λ, Equation 3) for the March TM image, further demonstrates this phenomenon with the large differences in average brightness between southern and northern slopes covered with a uniform deciduous forest canopy.

Plates 1(c) and 2(c) show that the topographic effect has been nearly completely removed with the second stage normalization, especially from the steeply sloping deciduous forests, while at the same time again preserving the overall spectral properties of the scene. Both of these observations are numerically supported by the data presented in Tables 2 and 3 for the March TM data, and Tables 4 and 5 for the May TM data. The data in Tables 2 and 4 indicate that the overall spectral reflectance properties (in terms of mean and variance) of the original TM data are preserved with either stage of the topographic normalization. However, Tables 3 and 5 reveal the additional improvement of the second stage transformation over the first stage version. While the mean spectral responses for the deciduous forest category for each level of transformation are nearly equal to those of the overall mean response of the original data, the within-category variance introduced by the topographic effect is substantially reduced in the second stage normalization. This effect is demonstrated graphically in Figures 1 (March TM data) and 2 (May TM data) which illustrate the degree of reduction of

TABLE 1. CALCULATION OF A CORRECTION COEFFICIENT C_λ TO BE USED IN SECOND STAGE NORMALIZATION.

Band	μ_λ	N_λ	N'_λ	S_λ	S'_λ	C_λ
1	80.9	76.8	83.5	84.8	77.7	0.58
2	30.8	28.6	30.7	34.1	30.9	1.04
3	41.0	36.0	38.9	48.0	43.7	1.68
4	51.7	45.4	49.0	60.5	55.3	1.72
5	99.8	81.6	88.6	124.4	114.3	2.52
7	43.9	35.5	38.3	56.0	51.1	2.73

μ_λ = the overall mean for the deciduous forest category
N_λ = the mean on northern slopes in the uncalibrated data
N'_λ = the mean on northern slopes after the *first stage normalization*
S_λ = the mean on southern slopes in the uncalibrated data
S'_λ = the mean on southern slopes after the *first stage normalization*
C_λ = the correction coefficient for band λ

$$= \frac{[(\mu_\lambda - n_\lambda)/((\mu_\lambda - N_\lambda) - (\mu_\lambda - N'_\lambda)) + (\mu_\lambda - S_\lambda)/((\mu_\lambda - S_\lambda) - (\mu_\lambda - S'_\lambda))]}{2}$$

TABLE 2. MEANS AND STANDARD DEVIATIONS FOR THE ENTIRE STUDY AREA FOR THE 24 MARCH 1987 TM DATA.

	Untransformed		First Stage Normalization		Second Stage Normalization	
Band	μ	σ	μ	σ	μ	σ
1	81.3	8.18	80.8	8.15	80.9	8.21
2	31.4	5.64	31.0	5.63	31.0	5.63
3	40.6	9.98	40.1	9.86	40.1	9.93
4	52.3	11.35	51.8	11.09	51.7	11.16
5	90.4	21.64	89.7	20.90	89.4	20.87
7	40.3	10.65	39.8	10.31	39.6	10.35

μ = overall scene mean (n = 157,451 pixels)
σ = overall scene standard deviation

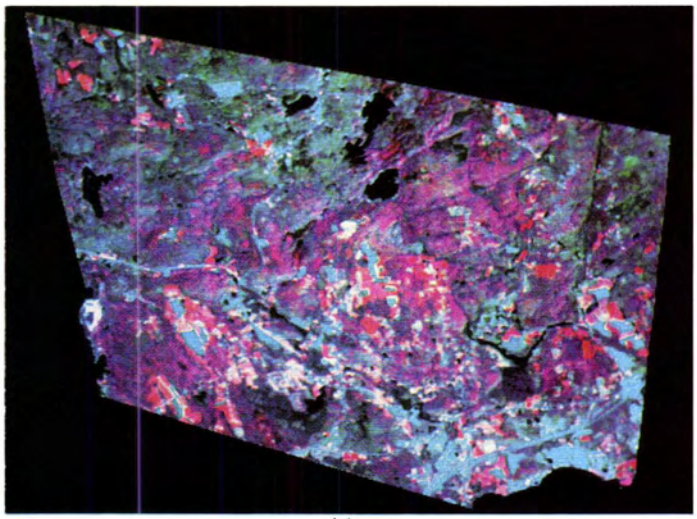

(a)

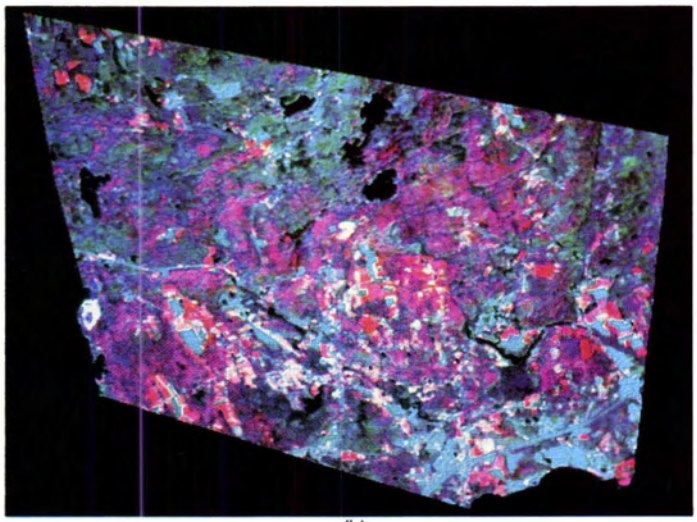

(b)

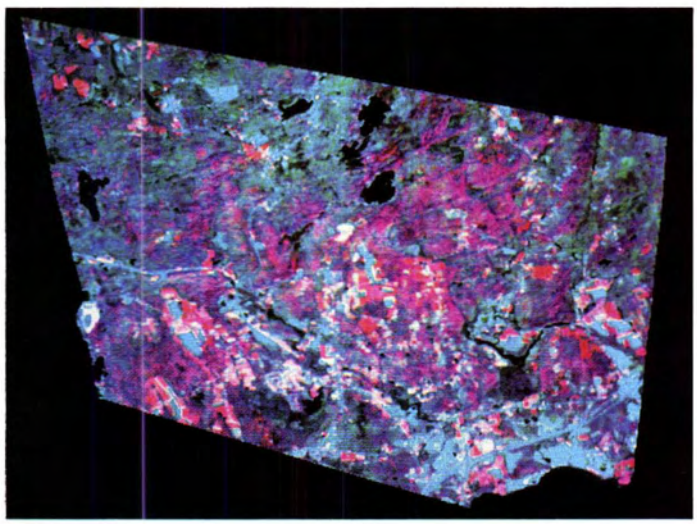

(c)

PLATE 1. Landsat TM Bands 2, 3, and 4, 24 March 1987, North Stonington, Connecticut. (a) Original image. (b) Result of first stage normalization. (c) Result of second stage normalization. Note the uniformity in brightness of deciduous forests on various slope-aspect combinations in (c), especially in the northwestern portion of the image. (EOSAT image copyright 1987. Scene ID 85111814401X0.)

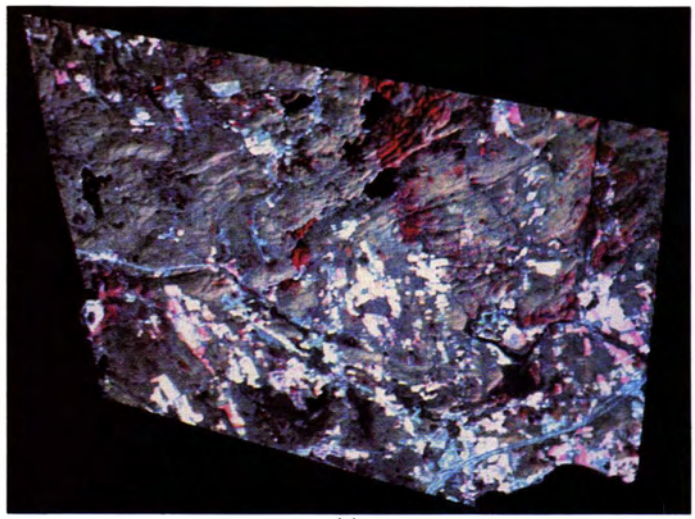

(a)

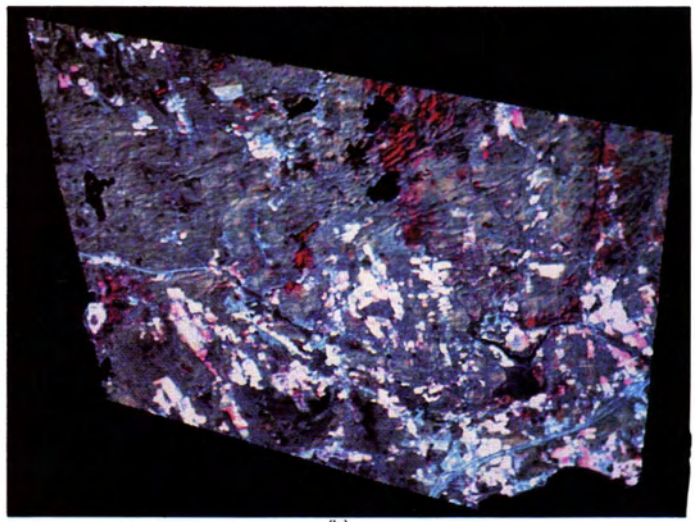

(b)

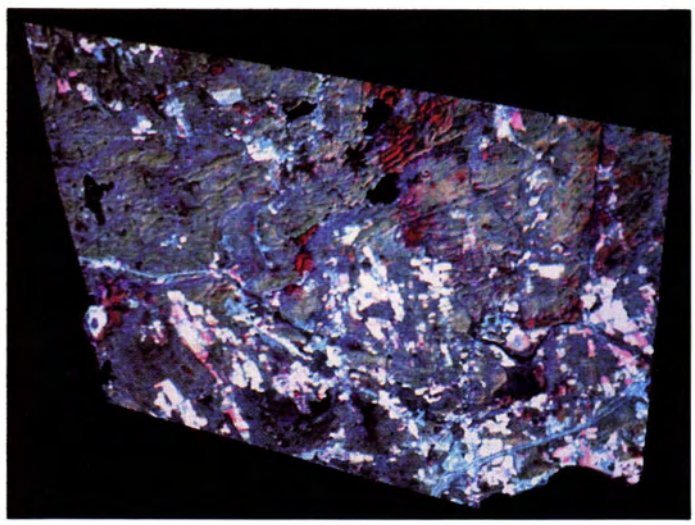

(c)

PLATE 2. Landsat TM Bands 2, 3, and 4, 11 May 1987, North Stonington, Connecticut. (a) Original image. (b) Result of first stage normalization. (c) Result of second stage normalization. Note the uniformity in brightness of deciduous forests on various slope-aspect combinations in (c), especially in the northwestern portion of the image. (EOSAT image copyright 1987. Scene ID 85116614504X0.)

TABLE 3. MEANS AND STANDARD DEVIATIONS FOR THE DECIDUOUS FOREST COVER CLASS FOR THE 24 MARCH 1987 TM DATA.

	Untransformed		First Stage Normalization		Second Stage Normalization	
Band	μ	σ	μ	σ	μ	σ
1	80.9	4.34	80.2	2.23	80.3	1.93
2	30.8	3.02	30.8	1.36	30.7	1.35
3	41.0	6.37	41.0	3.37	40.9	2.51
4	51.7	7.88	51.8	3.97	51.8	2.70
5	99.8	22.24	100.6	14.30	99.1	7.14
7	43.9	10.60	44.3	7.03	43.4	3.34

μ = mean for deciduous forest cover class sample (n = 2780 pixels)
σ = standard deviation for decidous forest cover class sample

TABLE 4. MEANS AND STANDARD DEVIATIONS FOR THE ENTIRE STUDY AREA FOR THE 11 MAY 1987 TM DATA.

	Untransformed		First Stage Normalization		Second Stage Normalization	
Band	μ	σ	μ	σ	μ	σ
1	100.0	6.75	99.7	7.04	99.6	6.83
2	41.4	4.44	41.0	4.52	41.0	4.47
3	42.7	8.12	42.3	8.14	42.2	8.37
4	87.1	15.05	86.7	14.98	86.6	14.99
5	95.4	18.09	95.0	17.80	95.0	18.31
7	36.4	10.78	36.0	10.71	36.0	11.13

μ = overall scene mean (n = 157,451 pixels)
σ = overall scene standard deviation

TABLE 5. MEANS AND STANDARD DEVIATIONS FOR THE DECIDUOUS FOREST COVER CLASS FOR THE 11 MAY 1987 TM DATA.

	Untransformed		First Stage Normalization		Second Stage Normalization	
Band	μ	σ	μ	σ	μ	σ
1	100.3	3.13	101.0	3.03	100.6	1.64
2	41.3	1.68	41.3	1.11	41.1	0.90
3	43.5	4.87	43.3	2.98	43.8	2.02
4	87.0	2.43	87.7	4.19	86.7	2.28
5	106.9	17.18	107.1	12.45	108.5	6.75
7	40.6	8.79	40.2	7.01	40.7	3.76

μ = mean for deciduous forest cover class sample (n = 2780 pixels)
σ = standard deviation for deciduous forest cover class sample

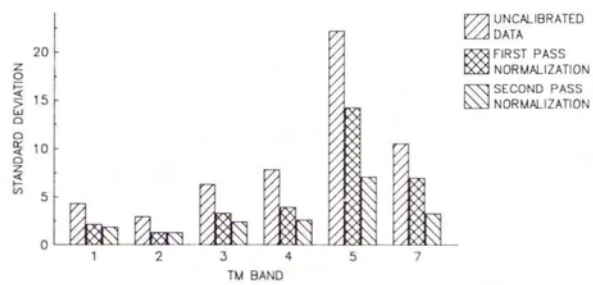

FIG. 1. Change in variance of spectral response from the uniform deciduous forest cover class after first and second stage normalization of the 24 March 1987 TM data.

within-category variance contained in the original TM data by each of the two stages of topographic normalization.

The data in Tables 3 and 5 and in Figures 1 and 2 reveal that variance in spectral response for the uniform deciduous forest

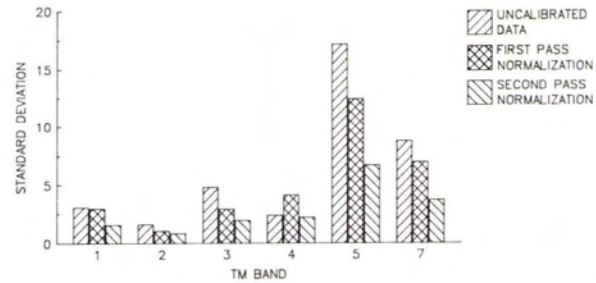

FIG. 2. Change in variance of spectral response from the uniform deciduous forest cover class after first and second stage normalization of the 11 May 1987 TM data.

cover was reduced by as much as 69 percent for the March image and 61 percent for the May image after application of the second stage normalization. While variance was similarly reduced in the first stage correction,[3] the topographic normalization proved to be inadequate as cited previously. This is illustrated by comparing the mean spectral responses from northerly and southerly facing aspects for deciduous forest (Table 6).

An additional test of improving overall scene characteristics by way of the second stage topographic normalization involved the application of a parametric unsupervised classification to each of the three images -- the *raw*, the first stage normalization, and the normalization involving empirically-derived coefficients. These unsupervised classifications resulted in the indentification of 42, 36, and 32 spectrally separable clusters. The fewer clusters identified in the second stage normalized image bore more resemblance to the number of informational classes in the TM data and produced a more comprehendable, uniform, classification map than did either the untransformed or first stage normalized images. In such an image where spectral variance is function of the actual cover classes themselves, rather than that introduced by topography, image segmentation based on spectral uniformity will be enhanced as will supervised classifications.

While the application of an empirically derived correction coefficient in the reduction of the topographic effect improved both the numerical and cosmetic properties of the Landsat TM data, it is recognized that it is an inherently scene-introspective calibration process. That is, C_λ, as described in this paper, is specific to different images and unique values must be generated accordingly. It is hypothesized that these spectrally dependent coefficients are a function of both the atmospheric scattering and the magnitude of radiant energy associated with each of the six Thematic Mapper reflective bands. In an attempt to model C_λ in terms of physical radiation principles, the relationship between this coefficient and a combination of atmospheric scattering and at-surface irradiance was examined.

Relative per-band atmospheric scattering for a Rayleigh sky (Chavez, 1988) was normalized to Landsat TM Band 2 -- the band with the least pronounced topographic effect. The inverse of this relative scattering coefficient was multiplied by the estimated within-band, at-surface irradiance, again normalized to TM Band 2. Estimated within-band, at-surface irradiance was calculated by modifying solar exoatmospheric irradiances (Markham and Barker, 1986) by the solar irradiation curve at sea level (Schanda, 1986). These data are presented in Table 7.

While the estimated topographic normalization calibration

[3] With the exception of Band 4 in the May TM data. Inexplicably, the within-forest category variance after first stage topographic normalization increased.

TABLE 6. MEAN SPECTRAL RESPONSES FOR DECIDUOUS FOREST ON NORTHERN AND SOUTHERN ASPECTS.

	24 March 1987 TM Data				11 May 1987 TM Data			
	First Stage Normalization		Second Stage Normalization		First Stage Normalization		Second Stage Normalization	
Band	Northern Aspect μ	Southern Aspect μ	Nothern Aspect μ	Southern Aspect μ	Northern Aspect μ	Southern Aspect μ	Northern Aspect μ	Southern Aspect μ
1	79.0	81.6	80.2	80.5	102.9	98.8	100.6	100.7
2	30.6	30.9	30.7	30.8	41.7	40.9	40.1	41.4
3	38.7	43.7	40.7	41.2	40.9	46.0	43.9	43.8
4	49.0	55.3	51.8	51.9	90.8	84.1	86.8	86.8
5	88.4	114.5	98.9	99.3	96.4	119.3	108.7	108.3
7	38.2	51.2	43.4	43.4	34.1	47.1	41.2	40.3

μ = mean spectral response for deciduous forest cover class sample (n = 2780 pixels)

TABLE 7. PRELIMINARY MODEL TO EXPRESS C_λ AS A FUNCTION OF AT-SURFACE IRRADIANCE AND ATMOSPHERIC SCATTERING.

Band	ρ	$1/\rho$ (A)	$ESUN_\lambda$	$ESUN'_\lambda$	$1/ESUN'_\lambda$ (B)	Estimated C_λ
1	18.07	0.56	195.7	138.5	1.09	0.61
2	10.17	1.00	182.9	127.3	1.00	1.00
3	5.27	1.93	155.7	118.6	0.93	1.79
4	2.11	4.82	104.7	65.4	0.51	2.46
5	0.14	72.64	21.9	16.3	0.13	9.44
7	0.04	254.25	7.5	4.9	0.04	10.17

ρ = relative scattering (Chavez, 1988)
$1/\rho$ = inverse of ρ relative to Band 2
$ESUN_\lambda$ = exoatmospheric irradiance (Markham and Barker, 1986)
$ESUN'_\lambda$ = estimated at-surface irradiances (*cf.* Schanda, 1986)
$1/ESUN'_\lambda$ = inverse of $ESUN'_\lambda$ relative to Band 2
Estimated C_λ = A × B

coefficient bears some resemblance to the elementary model considering relative atmospheric scattering and within-band, at-surface irradiances, the trend is not linear. A regression analysis between the empirically-derived coefficients and the ones derived through this elementary model indicated that the relationship can be described by a logarithmic function (R^2 = 0.97): i.e.,

$$C_\lambda = 1.0549 + 0.7209 \times \ln(\text{estimated } C_\lambda). \quad [5]$$

Additional research involving a number of scenes with different illumination, surface cover, and topographic characteristics is required, however, both to confirm and better define this relationship.

CONCLUSIONS

It is apparent that the technique described in this paper lends itself to the reduction of the topographic effect and to improvement of the overall multipectral image analysis and classification process. Based on this research, it can be concluded that

- the magnitude of spectral response (i.e., brightness) from a uniform cover type, such as deciduous forest, is topographically dependent;
- this topographic effect can be removed by normalizing the satellite radiance data with digital elevation data and a corresponding solar irradiance (i.e., shaded relief) model;
- a first pass correction of the original spectral data is inadequate;
- the magnitude of the topographic effect is also spectrally dependent, with greater corrections being required for the Thematic Mapper infrared bands;
- a scene-specific calibration coefficient can be derived and applied to uncorrected satellite radiance data as part of a second stage normalization that further removes the topographic effect while at the same time preserving an image's overall spectral properties; and
- there appears to be a relationship between this calibration coefficient and physical radiation properties.

In summary, the reduction of the topographic effect in Landsat Thematic Mapper data during the preprocessing phases of land-cover and land-use classification is envisioned as improving the overall computer-assisted mapping process.

ACKNOWLDEGMENTS

The research upon which this paper is based is supported, in part, by the Storrs Agricultural Experiment Station, The University of Connecticut, Storrs, CT, under Project 569, *Improved land cover mapping through innovative computer-assisted processing of satellite digital remote sensing imagery*. SAES Scientific Contribution Number 1279.

REFERENCES

Chavez, P. S., Jr., 1988. An improved dark object subtraction technique for atmospheric scattering correction of multispectral data. *Remote Sensing of Environment* 24:459–479.

Cicone, R. C., W. A. Malila, and E. P. Crist, 1977. *Investigation of the Techniques for Inventorying Forested Regions*. Final Report, Forestry Information and Systems Requirements and Joint Use of Remotely Sensed and Ancillary Data. NAS-CE-ERIM 122700-35-F2. Volume 2. 146 p.

Civco, D. L., 1987. *Knowledge-Based Classification of Landsat Thematic Mapper Digital Imagery*. Doctoral Dissertation. Department of Plant Science, The University of Connecticut, Storrs, Connecticut, 214 p.

———, 1989. Knowledge-based land use and land cover mapping. *Proceedings of the Annual Meeting of the American Society of Photogrammetry and Remote Sensing*, Baltimore, Maryland, pp. 276–291.

Civco, D. L., and W. C. Kennard, 1988. *Improved Land Cover Mapping through Innovative Computer-Assisted Processing of Satellite Digital Remote Sensing Imagery*. Storrs Agricultural Experiment Station Research Project, The University of Connecticut, Storrs, Connecticut.

Hall-Konyves, K., 1987. The topographic effect on Landsat data in gently undulating terrain in southern Sweden. *International Journal of Remote Sensing* 8(2):157–168.

Holben, B. N., and C. O. Justice, 1980. The topographic effect on spectral response from nadir pointing sources. *Photogrammetric Engineering and Remote Sensing* 46(9):1191–1200.

Jones, A. R., J. J. Settle, and B. K. Wyatt, 1988. Use of digital terrain data in the interpretation of SPOT-1 HRV multispectral imagery. *International Journal of Remote Sensing* 9(4):669–682.

Kawata, Y., S. Ueno, and T. Kusaka, 1988. Radiometric correction for atmospheric and topographic effects on Landsat MSS images. *International Journal of Remote Sensing* 9(4):729–748.

Leprieur, C. E., J. M. Durand, and J. L. Peyron, 1988. Influence of topography on forest reflectance using Landsat Thematic Mapper

and digital terrain data. *Photogrammetric Engineering and Remote Sensing* 54(4):491–496.

Markham, B. L., and J. L. Barker, 1986. Landsat MSS and TM post-calibration dynamic ranges, exoatmospheric reflectances, and at-satellite temperatures. *Landsat Technical Notes*. EOSAT, Lanham, Maryland, 1:3–8.

Schanda, E., 1986. *Physical Fundamentals of Remote Sensing*. Springer-Verlag, New York. p. 56.

Sellers, W. D., 1972. *Physical Climatology*. University of Chicago Press, Chicago, Illinois, pp. 33–37.

Shasby, M., and D. Carneggie, 1986. Vegetation and terrain mapping in Alaska using Landsat MSS and digital terrain data. *Photogrammetric Engineering and Remote Sensing* 52(6):779–786.

Teillet, P. M., B. Guindon, and D. G. Goodenough, 1982. On the slope-aspect correction of multispectral scanner data. *Canadian Journal of Remote Sensing* 8(2):84–106.

Woodcock, C. E., A. H. Strahler, and T. L. Logan, 1980. Stratification of forest vegetation for timber inventory using Landsat and collateral data. *Proc. 14th International Symposium on Remote Sensing of Environment*, ERIM, Ann Arbor, Michigan, pp. 1769–1787.